Bone Surface Model Development Based on Point Clouds Extracted from CT Scan Images

I. Asheghi Bonabi
Department of Mechanical Engineering,
University of Hormozgan, Iran
E-mail: iasheghi@yahoo.com

S. J. Hemmati*
Department of Mechanical Engineering,
University of Hormozgan, Iran
E-mail: hemmati@hormozgan.ac.ir
*Corresponding author

Abstract: In the present study a procedure is proposed for the development of bone surface models by using point clouds that can be extracted from CT scan images. Since the images are as multiple two dimensional sections, three methods of surface fitting are considered: ruled, skinning and global approximation methods. The required algorithms were discussed in fields of image processing and curve and surface fitting. For the purpose of further exploring the modelling requirements and results, and gaining further insights into the impacts of effective parameters, a computer program was developed. By adopting a detailed case study and analysis approach, three samples of the cattle's bones were selected and scanned with CT scan. Similar protocols corresponding to the human body bones were used during the scanning process. Subsequently, the surface models of the sample output from the program were transferred to CAD software. Moreover, the samples were scanned with COMET5™ scanner after removing the flashes surrounding the bones. It was observed that although the bone surface modelling is feasible within 0.25 and 0.75 mm accuracy range with these algorithms, skinning method works better compared to other two algorithms in terms of processing speed and increasing the ratio of data compaction. The use of control points balance algorithm and smoothing the contours, used in this paper, will greatly improve the performance of the program as well.

Keywords: Computer aided design, CT scan image, Digitizing, Point cloud, Surface modelling

Biographical notes: I. Asheghi Bonabi received his MSc in Mechanical Engineering from University of Hormozgan 2014. His current research interest includes Rapid prototyping. **S. J. Hemmati** is Assistant Professor of Mechanical engineering at the University of Hormozgan, Iran. He received his PhD in Mechanical engineering from Tarbiat Modares University of Iran and a BSc in Manufacturing from the University of Tabriz, Iran. His current research focuses on Computer Aided Design and Manufacture.

1   INTRODUCTION

In tomography, the kind of images are used which are provided from X-ray beams that are further transmitted or reflected from the object. In computed tomography (CT), a computer is used for data processing of these images. CT scans were first invented for the medical applications, but they were then generalized to the industry. In medical applications, CT scans are applied for diagnosis of glands, lung and liver, heart imaging, endoscopy, etc. [1]; while industrial CT scans are generally used for non-destructive tests, density measurement of materials, assembly inspection, engineering metrology and reverse engineering [2]. The result of processing involves surface/solid representation or modeling of tacit information of the CT images.

In Bio-CAD field, three dimensional (3D) displays of organs are mainly achieved by using either surface triangulation or solid representation methods. In the first method, dimensions of CT scan data are extracted from 2D segmentation [3-6]. Segmentation of images is usually performed by one of the following methods [7]: threshold methods, region based methods and boundary/surface based methods. Each image is individually processed for contour extraction of bone regions. Contours are saved into the 3D form and triangulated for 3D representation. Second method works via voxel accumulation. In this method, the reconstruction is done through algorithms like marching cube algorithm [8], [9]. Both of these methods have some reservations; for instance, in the first method, 3D surfaces reconstructed from contours is too extensive for dealing with discrete points of the contours, and in the second approach, voxel accumulation needs large computer capacity and there is no topological relationship. In surface modeling field, different algorithms including B-Spline, Loft and Sweep surface algorithms have been proposed for surface fitting over point clouds [10-13]. Among them NURBS (Non-Uniform Rational B-Spline) surfaces have gained a lot of interest due to their advantages. Ma and Kruth [14] have proposed an algorithm for curve and surface fitting of NURBS which automatically recognizes the control points and weights. Piegl and Tiller [15] randomly parameterized the points and developed an algorithm for NURBS surface fitting. They also addressed the difficulties of parameter values determination. Moreover, Yuwen et al., [16] suggested a technique for parameterization of B-Spline surface fitting and a strategy for point distribution in design techniques by using sectional images. They connected the initial boundaries of the curves by using a skinned surface after direct extraction of sectional contours from point clouds.

The present study aims to investigate the requirements of surface modelling based on information of the CT images. By segmentation different regions of CT images, it would be possible to achieve point clouds of body organs. Such point clouds can be used for visual investigation of the organs or tumors. Triangulation of the points situated on the external sides of the organs leads to a 3D grid, as it has been done in a number of earlier references; however, elimination of segmentation noises would not be an easy task. Furthermore, different advantages of geometrical models cannot be exploited. Therefore, in this paper, the requirements of surface modelling will be investigated and three different methods including ruled, skinning and global approximated surface fitting would be compared. There is no report of using Ruled and Global methods for surface modelling in this context. In addition, there is no reference to using smoothing algorithms or control points balance for surface modelling in previous studies.

2   CALCULATIONS

Fig. 1 represents the flow diagram of different steps of surface modeling used here. Input data are a number of CT images. In the loop with parameter of i which starts from 1 to the number of CT images, the content of ith image is evaluated and the bone regions are recognized. "Region growing" method, which is one of the segmentation methods based on the region [17], was used to segment bone regions. This method is applicable for images in which internal pixels of each region have similar intensities. Initially, a number of points are selected as seed points. Then neighbor points are investigated and pixels which have similar properties to the seed points (such as color intensity) are included in the region. This step is repeated until no point is added to the region and no growth is observed in the target regions. The syntax for the corresponding function is as:

regiongrow (image, seed, threshold)

Where seed parameter defines an intensity value such that all the points with that value would be regarded as seed points. The threshold value is used to test if a pixel in the image is sufficiently similar to the seed to which it is 8-connected or not. The segmented image with the members of each region is an output of the function. Fig. 2 represents a typical CT scan image and the results of segmentation. After bone-region recognition, external boundaries would be determined in the form of closed curves of boundary pixels (contours). This step is known as edge detection. For this purpose, a threshold is needed to determine internal and external pixels of the region. Analysis of histogram of the image is one of the proper methods. In this method, intensity

of the most amplitude is selected as threshold. The syntax of the function is as:
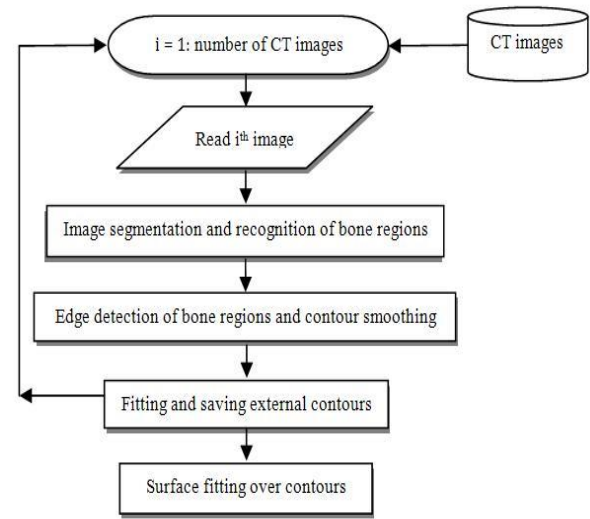

Fig. 1   Flow diagram of surface modeling procedure

(a)   (b)   (c)
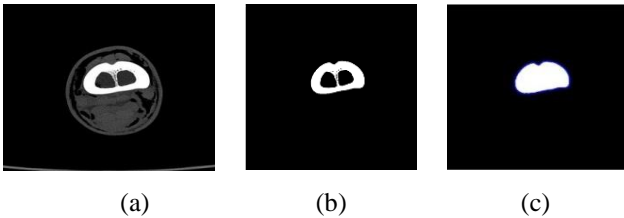
Fig. 2   (a) A typical CT scan image, (b) segmentation of bone region, (c) bone section without internal parts

Edge-detection (region, threshold (histogram (region))) where region describes each region extracted already. Fig. 2C shows main region without internal parts. Output of the function is a contour of the region. Since pixels are in the form of squares, the contours will be crenate. Since no segments of natural bone can be crenate and discontinuous, a smoothing step is applied over the contour to make it finally C^2 continuous. The algorithm of Hemmati-Derakhshan [17] is used for contour smoothing.

Regarding Fig. 3, it is assumed that using a mathematical support and impact, P_2 is smoothed between P_1 and P_3. The proposed algorithm is as follows: a) if P_i, P_{i+1} and P_{i+2} are three sequential pixels on contour (where i = 0, 1... m and m is the total number of pixels), then x and y coordinates of P_{i+1} is calculated as mean of the coordinates of P_i and P_{i+2}. b) P_{m+2} equal to P_0 is added to the set of pixels since at the beginning, the first and last pixels coincide with each other, because the contour is closed. This cycle is repeated in a loop till the desirable smoothness is obtained. Experiences show adequate smoothness is

obtainable by three times repeating of the cycles. Fig. 4 represents an example of smoothed contours.

Fitting of NURBS curve would be performed after extracting the smooth contour of bone-region for the ith image. Fitted curve may not pass through all pixels due to noises in the contour. It should have the dominant shape of contour and be suitably continuous. To achieve this, the least square method of Piegl and Tiller [18] is used for the curve approximation. In this method, user determines degree of the curve and maximum allowable error over pixels of the contour. The assumption is that the degree of fitting curve ($\equiv$ p) $\geq$ 1 and number of its control points ($\equiv$ n+1) $\geq$ p, and also Q_0, Q_1, …, Q_m (m > n) are given pixels. To avoid the nonlinearity problem, we set the weights of control points to unit. We seek a curve as:

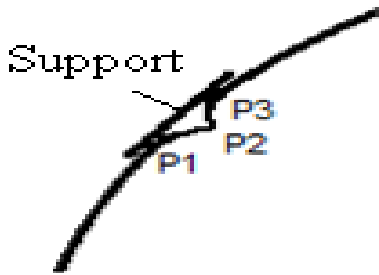$$C(u) = \sum_{j=0}^{n} N_{j,p}(u)p_j, \qquad u \in [0,1] \qquad (1)$$

Fig. 3   Schematics of smoothing method
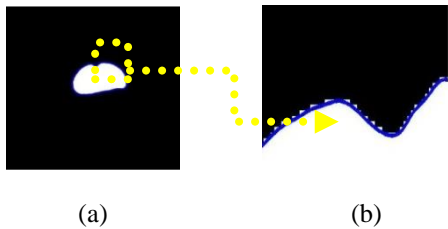

(a)   (b)

Fig. 4   (a) External contour of bone region, (b) Enlarged view of a smoothed contour part

Satisfying that $Q_0= C(0)$ and $Q_m= C(1)$, and the remaining Q_k are approximated in the least squares sense, i.e. $C(u) = \sum_{k=1}^{m-1}\left|Q_k - C(\bar{u}_k)\right|^2$ is a minimum with respect to the $n+1$ variables P_i (control points). $N_{j,p}(u)$ are B-Spline functions. Centripetal method was applied for calculation of the parameters $\{\bar{u}_k\}$. Let

$$d = \sum_{k=1}^{n} \sqrt{\left|Q_k - Q_{k-1}\right|} \qquad (2)$$

Then

$$\overline{u}_0 = 0, \quad \overline{u}_m = 1, \quad \overline{u}_k = \overline{u}_{k-1} + \left(\sqrt{|Q_k - Q_{k-1}|}\Big/d\right), \quad k = 1, 2, ..., m-1 \quad (3)$$

In fact, we set up and solve the linear least squares problem for the unknown control points. In this case a knot vector as U= {u_0, u_1… u_r} is required. The placement of the knots should reflect the distribution of the {$\overline{u}_k$}. If D is a positive real number, denote by i= int (D), the largest integer such that i ≤ D we need a total of $n+p+2$ knots; there are n-p internal knots, and n-p+1 internal knot spans. Let $D = (m+1)/(n-p+1)$, then the internal knots are defined by

$$i = \text{int}(jD), \quad \alpha = jD - i \quad (4)$$

$$u_{p+j} = (1-\alpha)\overline{u_{i+1}} + \alpha\overline{u_i} \quad j = 1, ..., n-p \quad (5)$$

Fig. 5 shows the fitted curve over the contours extracted from three sequential images. Dots in the figure indicate the control points of the fitted curves. Surface fitting can be implemented for the curves. In this case ruled, skinning and global approximation algorithms can be used since all of these methods work based on the sectional curves. Figures 6 to 8 represent the typical NURBS curves and indicate the results of surface fittings. In ruled method (Fig. 6), degree of the surface in direction of the initial sections is equal to degree of the fitting curves, but its degree in perpendicular direction (longitudinal direction) is one, since the sectional curves are connected to each other by lines. In the skinning method (Fig. 7), control points of fitted surface are the same as the control points of fitted curves, and degree of the surface can be selected in both directions (sectional and longitudinal directions). For global approximated surfaces (Fig. 8), boundary control points are fixed, but those inside the network of control points of sectional curves are variable. To model these surfaces, we used corresponding algorithms from [18].
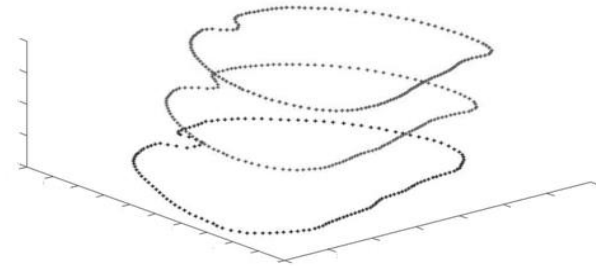

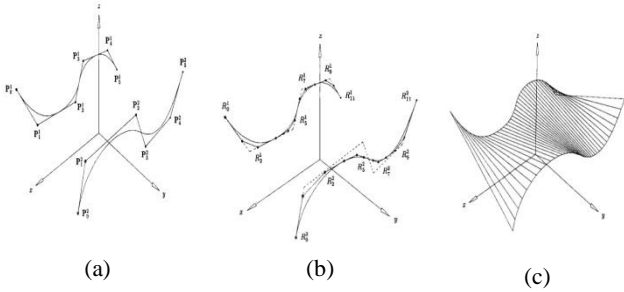**Fig. 5**   Control points of three fitted curves corresponding with sequential contours

Fig. 6   (a) Two sectional curves with their control polygons, (b) curves after knot refinement, (c) resultant ruled surface [18]
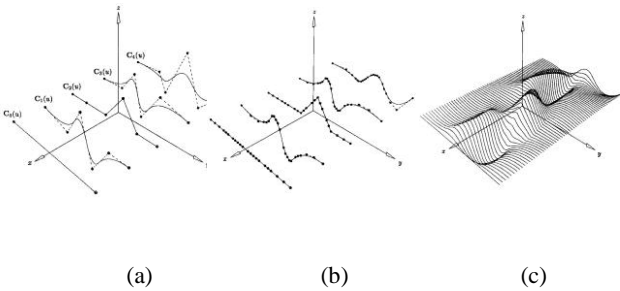

Fig. 7   (a) Five sections with their control polygons, (b) sections after knot refinement, (c) resultant skinned surface [18]
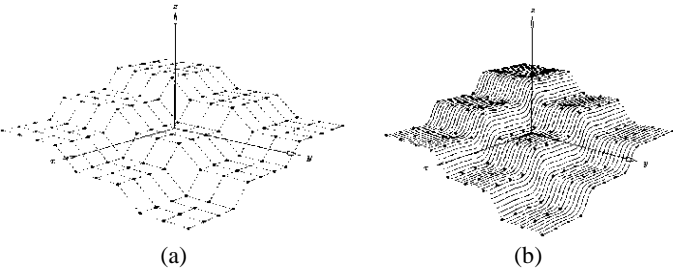
Fig. 8   (a) Thirteen 10-point network of data points, (b) resultant global approximation [18]

It should be noted that in all these methods, sectional curves should have the same "number of control points" (NCP) and degree. Therefore, "knot refinement" process is necessary before surface fitting [18]. For this purpose, all knots in knot vector of sectional curves were saved in an array (as a global knot vector). Then knot vector of each curve was conventionally compared with the global knot vector and added to the knots which were not available in the knot vector.

(a)   (b)

(c)

Fig. 9   (a) First sample during CT scan, (b) Second sample before and after removing its flash tissues, (c) Third sample without surrounding flash tissue
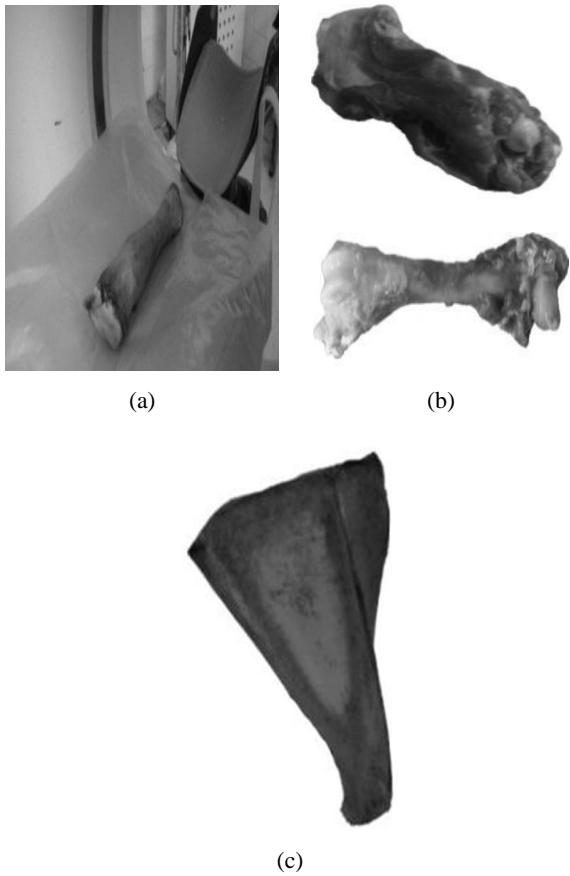

(a)   (b)

(c)

Fig. 10   Fitted surfaces for samples of Fig. 9 by skinning method

Finally, all knot vectors were equalized which would make the fitting of the surface possible. Addition of extra knots involves a "knot insertion" process [18]. Aggregation of close knots in knot vector leads to oscillating of the curve in corresponding portions and decreasing of curve smoothness. Therefore, here, a tolerance was applied to reduce these knots to a mean value. This is called balancing of the control points.

3   RESULTS

A computer program was developed based on the aforesaid algorithms. To verify the program three bones of cattle and sheep were investigated with their surrounding flash tissues. The samples were radiated by 16-slice Spiral Siemens CT scan.
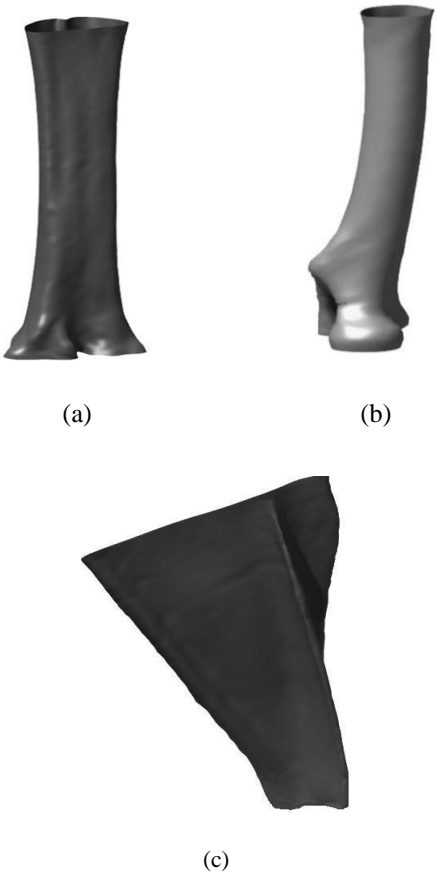

(a)   (b)

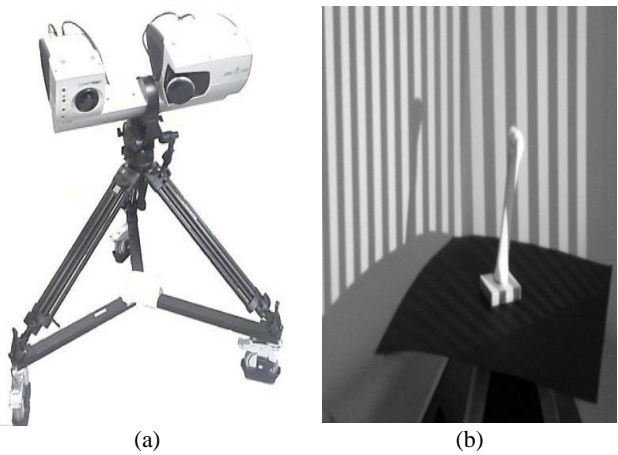**Fig. 11**   (a) The COMET5^{TM} scanner, (b) 3D scanning for the second sample

(a)   (b)

Fig. 12   (a) Point clouds of COMET5™ scanner,
(b) consistency of point clouds with output of the developed
program as a color coded image

Scan parameters were selected based on the protocols similar to the bones of human body. Fig. 9 represents the samples. Fig. 10 shows the skinned surfaces fitted on the samples. The samples were also scanned with COMET5™ scanner after removing their surrounding flash tissues (Fig. 11).

Tabel 1   The design parameters of first test

NCP	$\mu+3\sigma$ (mm)	Control points balancing tolerance (mm)	Curve fitting Tolerance (mm)	Threshold for segmentation	Surface fitting method [i]	Sample No.	Curve degree in section direction
11390	0.3199	0.010	0.15	145	R	1	2
9240	0.3779	0.015	0.30	150	S	1	2
129168	0.5281	0.020	0.60	155	A	1	2
7928	0.3371	0.015	0.30	145	R	2	2
9800	0.4816	0.020	0.60	150	S	2	2
569058	0.3331	0.010	0.15	155	A	2	2
20438	0.5088	0.020	0.15	150	R	3	2
13800	0.6893	0.010	0.30	155	S	3	2
170082	0.6902	0.015	0.60	145	A	3	2
5476	0.5366	0.015	0.60	155	A	1	3
42280	0.3053	0.020	0.15	145	S	1	3
373838	0.3681	0.010	0.30	150	A	1	3
5204	0.488	0.010	0.60	150	R	2	3
29400	0.3042	0.015	0.15	155	S	2	3
328568	0.3653	0.020	0.30	145	A	2	3
14300	0.5703	0.020	0.30	155	R	3	3
11760	0.7655	0.010	0.60	145	S	3	3
5.2E+06	0.6592	0.015	0.15	150	A	3	3

[i]R: Ruled method, S: Skinning method and A: global

Point clouds of 3D CT scan were transferred to CAD software with STL format to be compared with the results of the developed program. For this purpose, point clouds of 3D scan were introduced as the reference; and mean deviation (μ), minimum, maximum and standard deviation (σ) were evaluated for three models. Fig. 12 shows the consistency of 3D scan results with output of the program as color coded.

Tabel 2   Design parameters of second test

NCP	$\mu+3\sigma$ (mm)	Image distance (mm)	Surface degree in perpendicular to section
13580	0.3844	1	2
13580	0.3844	1	2
13580	0.3844	1	2
2408	0.4002	5	2
2408	0.4002	5	2
2408	0.4002	5	2
1106	0.4359	10	2
1106	0.4359	10	2
1106	0.4359	10	2
13580	0.3810	1	3
13580	0.3810	1	3
13580	0.3810	1	3
2408	0.4094	5	3
2408	0.4094	5	3
2408	0.4094	5	3
1106	0.4493	10	3
1106	0.4493	10	3
1106	0.4493	10	3

Taguchi design of experiments was used for investigating the role of effective parameters on the quality of outputs. The considered parameters include: surface fitting method (ruled, skinning and global approximated surfaces), bone type (first, second and third sample), degree of fitted curves (second and third degrees), tolerance of segmentation, error of curve fitting, distance between sections, field of view (FOV), degree of the surface in longitudinal direction and tolerance of knot refinement. As it was mentioned before, although knot refinement makes surface fitting possible, it also increases NCP. Especially in the case of large number of curves, increase in NCP will lead to increase of the computational costs. Since this amount of computing does not have positive impact on the accuracy of final model, tolerance was applied to balance the control points. Indeed, the balancing of

control points by application of tolerance on the knot vector removes the adjacent knots. Variation of the tolerance, in addition to change in NCP, will change the accuracy of the final model. As a result, the role of this parameter should have been studied. The quality of fitted surface was defined by using two parameters including μ+3σ (as a measure of accuracy) and NCP (as the indicator of output data volume).

Tabel 3 Design parameters of third test

NCP	μ+3σ (mm)	FOV (mm)	Surface fitting method
19800	0.3603	80	S
19400	0.3401	105	S
618453	0.3879	80	A
619927	0.4641	105	A

Tabel 4 Design parameters of fourth test

NCP	μ+3σ (mm)	Image distance (mm)	Curve fitting tolerance (mm)
11426	0.2167	1	0.15
2250	0.3344	5	0.15
1028	0.5070	10	0.15
8184	0.2541	1	0.30
1622	0.3696	5	0.30
778	0.5280	10	0.30
5356	0.4284	1	0.60
1076	0.5066	5	0.60
520	0.6062	10	0.60

Tabel 5 Effect of curve smoothing application

NCP	μ+3σ (mm)	Surface degree in direction and perpendicular to sections	Smoothing	Surface fitting method
10806	0.3601	3,1	✗	R
15680	0.2744	3,3	✗	S
498512	0.2738	3,3	✗	A
8184	0.2541	3,1	✓	R
13580	0.2470	3,3	✓	S
230181	0.2485	3,3	✓	A

After comparing the results of experiments it was observed that the errors of surface fitting occur in some special limited regions so that minimum or maximum error cannot be considered as a complete criterion of surface accuracy. Moreover, these errors were

completely local, and selection of μ+3σ measure made it possible to discuss and investigate the accuracy of whole surface over 99.74% of points. By surface modeling, the memory occupied by CT images is replaced by a file containing the surface data, which is much smaller in volume. For evaluation of the compaction ratio, NCP was used as a parameter which has a direct relationship with the volume of output memory.

Tables 1 to 5 show the effective parameters with corresponding values of μ+3σ and NCP. Analysis of these tables with Taguchi method, signal to noise charts can be plotted for finding the effect of each input parameter. In the first test, the samples were investigated by three surface modelling methods with the parameters introduced in Table 1.
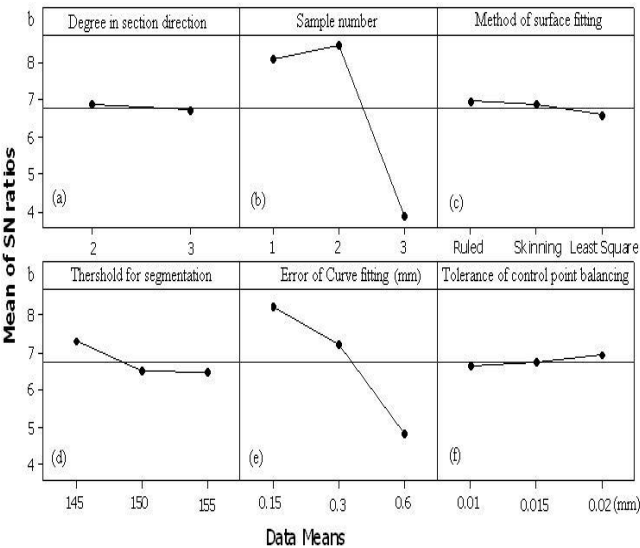

Fig. 13 Main effects plot for Signal to noise ratios of the first test

In the second test (Table 2) the fitting was done for the first bone sample with FOV of 100 mm and tolerance of curve fitting of 0.3 mm, by skinning method with degree of three in the direction of sections and balance tolerance of 0.01 mm for the control points. Number of CT images in this test was 140. In the third test (Table 3), quadratic surface fitting was performed with tolerance of 0.01 mm for balancing control points over 200 curves of second sample and the distance of 0.6 mm with fitting curve tolerance of 0.3 mm. In the fourth test (Table 4), ruled surface with balance tolerance of 0.01 mm was fitted over 140 curves of first sample with FOV and tolerance of curve fitting of 100 and 0.3 mm, respectively. In this test the degree of the sectional fitted curves was three. In order to investigate the effect of contour smoothing, 140 images of the first sample with FOV of 100 mm and tolerance of cubic curve fitting of 0.3 mm were used (see Table 5).

Fig. 13 represents the results of Taguchi method applied for the first test. After carrying out the test and measurements, results were analyzed using Minitab software. The presumption was that the lower error, the better. One of the outputs of Taguchi analysis is Signal to Noise (S/N) ratio. For each level of an effective parameter (and different values for the others), a value is determined as mean S/N ratio which indicates the impact level of the parameter. Each chart of Fig. 13 is related to changes in one of the input parameters. In the middle of these charts, a horizontal line is plotted indicating the influence of the input parameter on the output results. The higher slope related to the horizontal line means more importance of corresponding parameter.

4   DISCUSSION

Fig. 13(b) reveals that the most effective parameter for the accuracy of the output model is the sample number, so that the second sample has led to the highest level of accuracy. This finding can be attributed to the sample surface since it is smoother than the other samples. There are distortions in some regions of the first sample. The third sample has lower density and as a result, identification of the bone region will be more difficult. Furthermore, this sample has softer tissue in some regions and the tissue has ended to the cartilage. The second effective parameter is the applied tolerance during curve fitting. The curve can be seen in Fig. 13(e). As expected, by increasing the error from 0.15 mm to 0.3 mm and also from 0.3 mm to 0.6 mm, the dimensional accuracy of the model decreases. The increasing rate of errors from 0.3 to 0.6 mm is higher since the slope of the curve has increased.

The next effective parameter is the selected threshold in segmentation. As was previously mentioned, in the region growth algorithm two numbers are needed as input for the corresponding function: the intensity of seed points and the applied threshold through the image. Since in the present work the identification of bone region was important and in the CT scan images of high-density region is completely in white, the intensity of seed points was considered constant by the maximum value (255). However, the applied threshold over images has a significant effect in the results. For the first sample which was taken from the cattle with higher density, the threshold for segmentation can be selected from a wide range, but for other samples the selection was more limited. Considering the interface of these selections, values of 145, 150 and 155 were used. By studying Fig. 13 for the other input parameters, it can be seen that:

- Second order curves for fitting in the direction of sections have higher accuracy compared to the third order.
- The order of accuracy of the used methods is: ruled>skinning >global approximation.
- By increasing the applied tolerance during the balance of control points, accuracy enhances relatively.

As it is known, increasing the degree results in an increase in the distance between the curve and its control polygon. Therefore, the increase of extent of error by increasing the degree from two to three is not far from expectation. The ruled method has the highest accuracy and the skinning method is in the next rank. The degree of surface continuity in the ruled method is of the order of point continuity. In other word, the surface of the model is not smooth and it has some discontinuities leading to the weaker model appearance in comparison to the skinning method. A point worth mentioning is that the distance between images is low and such discontinuities cannot make errors. The reason for higher errors in the global approximation method can be attributed to the fact that in this method, curve fitting is done in longitudinal direction in addition to the sectional directions. Curve fitting algorithm works based on the maximum error and it can shift the error band. The reason of accuracy enhancement by tolerance increase is the decrease of NCP which consequently decreases the curve and surface distortion.

Knot refinement increases NCP significantly. In this case the increase of control points increases the effect of noises, leading to curve and surface distortion. Moreover, since these points have not been identified previously and the software should increase knots in knot vector, the error would increase.

For evaluation of input parameters for the first test on NCP in addition to data presented in Table 1, a figure similar to Fig. 13 can be proposed, which has been removed for briefness. The results indicate that NCP had significantly increased in global surface approximation. The minimum NCP is for the ruled method. Skinning method uses refinement process one time while global approximation method uses the knot refinement two times, increasing NCP much more. The second effective parameter is the applied error during curve fitting. By decreasing the maximum applied error during curve fitting, NCP increases. The next effective parameter is the degree of fitting curve. By increasing the degree from two to three, NCP increases. The other parameters have not significant effects on NCP. In the second test, the effects of distance between images and surface degree in longitudinal direction were investigated.

The results indicate that distance between images is an important parameter in estimating the accuracy of the model. The error would increase by raising the degree in longitudinal direction from two to three. This can be accounted for by the increase of the surface distance from data points by increasing the degree.

Increase of the distance between images in the unit length decreases the number of images and consequently fitted curves to decrease and drops NCP compared to similar condition. Since this test has been implemented by skinning method, change of surface degree does not have any effects on NCP in longitudinal direction.

The third test was intended to study the influence of FOV. Table 3 reveals that FOV has no significant effect on model accuracy. However, it is suggested that during reconstruction, the least possible value must be used for this parameter to achieve smaller pixel size. Also it can be seen that FOV has a low effect on NCP. Table 3 indicates that the type of modeling method can have an important impact on NCP. Since in this test FOV was investigated by different modeling methods, the effect is not that much considerable.

In the fourth test, the ruled method was applied. In this test the accuracy would be decreased by increasing the distance between the images from 1 to 10 mm. Also as the distance decreases, number of images and number of fitted curves increases, which further leads to the increase of control points.

The results of Table 5 indicate that smoothing reduces the error and NCP. This is especially very important in case of global approximation method, since in comparison with other methods, this method suffers from a higher NCP.

5   CONCLUSION

In the present study, the requirements of surface modeling were investigated based on the point clouds extracted from CT scan images. For this purpose, a program was developed in which three types of surfaces can be fitted over the point clouds of the bone regions. The results indicated that 99.74% of points on the reconstructed surfaces by the developed program have a maximum distance of $\mu+3\sigma$ from the reference data. This value is about 0.25 to 0.75 mm, which seems to be of an adequate level of accuracy for medical applications. Although by decreasing the distances between images, surface modeling by ruled method reaches more accurate results, the skinning method has more flexibility and accuracy in case of decreasing the number of images. It seems that global approximation method is not preferable to skinning and ruled methods due to the higher computational cost and process time.

Moreover, the roles of other effective parameters on accuracy of the surface and also volume of output data were estimated. The positive effect of contour smoothing method and balance of control points which were suggested by the authors were explained. It is expected that more suitable results could be achieved by application of curve fairing algorithm after curve fitting.

REFERENCES

[1] Subburaj, K., "CT Scanning Techniques and Applications", INTECH, 2011, chapt. 1.

[2] Chiffre, L., Camignato, S., Kruth, J. -P., Schmitt, R., and Weckenmann, A., "Industrial Applications of Computed Tomography", CIRP. Annals-Manufacturing Technology, Vol. 63, 2014, pp. 655-677.

[3] Sun, W., Starly, B., Nam, J. and Darling, A., "Bio-CAD Modeling and its Applications in Computer Ttissue Engineering," Comuter-Aided Design, Vol. 37, No. 11, 2005, pp. 1097-1114.

[4] Viceconti, M., Casali, M., Massari, B., Cristofolini, L., Bassini, S., and Toni, A., "The Standardized Femur Program Proposal for a Reference Geometry to be used for the Creation of Finite Element Models of the Femur", J. Biomech. Vol. 29, 1996, pp. 525-535.

[5] Viceconti, M., Zannoni, C., and Pierotti, L., "TRI2SOLID: an Application of Reverse Engineering Methods to the Creation of CAD Models of Bone Segments", Comput. Methods and Progr. in Biomed., Vol. 56, 1998, pp. 211-220.

[6] Lee, T. Y., Lin, C. H., "Feature-Guided Shape-Based Image Interpolation," IEEE Trans.on Med. Imaging, Vol. 21, 2002, pp. 1479-1489.

[7] Gonzalez, R. C., Woods, R. E., and Eddins, S. L., "Digital Image Processing Using Matlab", 2nd ed., Pearson Education., 2010, Chapt. 10.

[8] Rajon, D. A., Bolch, W. E., "Marching Cube Algorithm: Review and Trilinear Interpolation Adaptation for Image-Based Dosimetric Models. Comput", Med. Imaging and Graph., Vol. 27, 2003, pp. 411-435.

[9] Ma, D., Lin, F., and Chua, C. K., "Rapid Protyping Applications in Medicine Part 1: NURBS-Based Volume Modelling", Int. J. of Adv. Manuf. Technol.,Vol. 18, 2001, pp. 103-117.

[10] Yoo, D. J., "Three-Dimensional Surface Reconstruction of Human Bone using a B-spline Based Interpolation Approach", Comput. Aided Des., Vol. 43, 2011, pp. 934-947.

[11] Lai, J. Y., Ueng, W. D., "Reconstruction of Surface of Revolution from Measured Points", Comput. in Ind.,Vol. 41, 2000, pp. 147-161.

[12] Park, H., "An Approximate Lofting Approach for B-Spline Surface Fitting to Functional Surfaces", Int. J. of Adv. Manuf. Thechnol.,Vol. 18, 2001, pp. 474-482.

[13] Ueng, W. D., Lai, J. Y., and Doong, J. L., "Sweep-Surface Reconstruction from Three-Dimensional Measured Data", Comput. Aided Des.,Vol. 30, 1998, pp. 791-805.

[14] Ma, W., Kruth, J. P., "NURBS Curve and Surface Fitting for Reverse Engineering", Int. J. Adv. Manuf. Technol.,Vol. 14, 1998, pp. 918-927.

[15] Piegl, L. A., Tiller, W., "Parametrization for Surface Fitting in Reverse Engineering", Comput. Aided Des., Vol. 33, 2001, pp. 593-603.

[16] Yuwen, S., "B-spline Surface Reconstruction and Direct Slicing from Point Clouds", Int. J. Adv. Manuf. Technol.,Vol. 27, 2006, pp. 918-924.

[17] Derakhshan, A., "Automatic Extraction of the Machining Program from Raster Image", MSc Dissertation, Mech. Eng. Dept., Univ. of Hormozgan, 2013.

[18] Piegl, L. A., Tiller, W., "The NURBS Book", Berlin, Springer Press, 1997, chaps.5, 9, 10.